Energetics and Thermodynamic Stability of the Mixed Valence Ytterbium Germanides

ARTICLE *in* THE JOURNAL OF PHYSICAL CHEMISTRY B · JUNE 2007

Impact Factor: 3.3 · DOI: 10.1021/jp067889b · Source: PubMed

6 AUTHORS, INCLUDING:

Giovanni Balducci
Sapienza University of Rome
84 PUBLICATIONS **1,009** CITATIONS
SEE PROFILE

Andrea Ciccioli
Sapienza University of Rome
36 PUBLICATIONS **304** CITATIONS
SEE PROFILE

Guido Gigli
Sapienza University of Rome
79 PUBLICATIONS **995** CITATIONS
SEE PROFILE

Marcella Pani
Università degli Studi di Genova
141 PUBLICATIONS **816** CITATIONS
SEE PROFILE

Energetics and Thermodynamic Stability of the Mixed Valence Ytterbium Germanides

G. Balducci,[†] S. Brutti,*[,†] A. Ciccioli,*[,†] G. Gigli,[†] A. Palenzona,[‡] and M. Pani[‡]

Dipartimento di Chimica, Università di Roma-La Sapienza, P. le A. Moro 5,I-00185 Roma, Italy, and INFM, Dipartimento di Chimica e Chimica Industriale, Università di Genova, via Dodecaneso 31, I-16146 Genova, Italy

Received: November 28, 2006; In Final Form: February 22, 2007

The results of an experimental study concerning the thermodynamic stability of the Yb germanides, described as intermediate valence compounds, complemented by a computational investigation for the Yb_3Ge_5 compound are reported. These compounds belong to the rare earth (RE) tetrelides (tetrel = Si, Ge, i.e., group 14 elements), a class of intermetallic materials showing unusual and promising physical properties (giant magnetocaloric effect, magnetostriction, and magnetoresistence). The high-temperature decomposition reactions of the Yb−Ge intermediate phases were studied experimentally by means of the KEMS (Knudsen effusion mass spectrometry) and KEWL (Knudsen effusion weight loss) techniques. From the reaction enthalpies derived by measuring the Yb(g) decomposition pressures as a function of temperature, the heats of formation of five out of six of the intermediate phases in the Yb−Ge system were calculated. From the computational side, the stability of the Yb_3Ge_5(s) compound has been investigated by DFT-LCAO-B3LYP (density functional theory-linear combination of atomic orbitals-hybrid b3lyp exchange-correlation functional) first principles calculations deriving its equilibrium geometry and the enthalpy of formation at 0 K in relation to the intermediate valence state of Yb in the lattice.

1. Introduction

The mixed valence character of certain lanthanide atoms (e.g., Yb, Eu, Ce, Sm, and Tb) in several rare earth (RE) tetrelides (tetrel = Si, Ge) and its modulation via several parameters such as temperature, pressure, external magnetic field, and chemical composition have been reported to result in unusual and promising physical properties (giant magnetocaloric effect, magnetostriction, and magnetoresistence).[1] Indeed this behavior, that originates from the existence of two nearly degenerate electronic configurations of the lanthanide atoms in the lattice because of the 4f orbitals that lies close to the Fermi energy, could lead, for example, to temperature induced Yb valence change (from nonmagnetic divalent to magnetic trivalent configuration or vice-versa), so modifying the magnetic ordering of the lattice.[2] This fascinating basic solid-state phenomenon is therefore strongly related to possible challenging applications of these materials, for example, in the field of magnetic refrigeration.[1] However, in order to obtain a fine-tuning of the valence behavior of the RE in the lattice, driven syntheses are required. Indeed, as already mentioned, the electronic configurations realized by the composition modulation of a RE compound, for example, via anion or cation doping, could lead to continuous or abrupt induced valence transitions.[2−4] The attainment of the most suitable synthesis conditions can be driven on a thermodynamic basis starting from the knowledge of the stabilities of the relevant phases. However these data are often missing leading to serendipitously discovered try-and-fail synthesis routes.

Although Yb tetrelides show attracting potentialities as magnetic materials in view of the mixed valence character of several phases[5,6] or as contact materials in Si/Ge-wafer-based microelectronic devices,[7] the information on phase equilibria, crystal chemistry, and thermodynamic properties of intermediate phases is far from being satisfactory.[8] Grytsiv et al. studied the phase relations of the Si(Ge)-rich parts of the systems Yb−Si[9] and Yb−Ge[10] reporting the structure and physical properties of Yb_3Si_5 and Yb_3Ge_5 while Palenzona et al.[11] and Pani and Palenzona[12] determined the Yb−Si and Yb−Ge phase diagrams in the whole composition range. The current phase diagram is presented in Figure 1. New compounds such as Yb_5Si_4, Yb_3Si_4, Yb_5Ge_4, and Yb_3Ge_8 have been found and completely characterized. Parallel and concomitantly to these investigations our efforts were directed to measure the hitherto missing thermochemical data for the formation of the intermediate phases. Apparently, in fact, thermodynamic data, although incomplete, were reported previously only for Yb plumbides and stannides.[13] In their critical assessment of the thermodynamic data for RE-IV group p element intermetallics, Witusiewicz et al. remark how experimental difficulties in the electromotive force (emf) and calorimetric investigations of these systems at high temperatures are somewhat responsible for the incompleteness of data. This is particularly true for Yb compounds. After the thermodynamic characterization of the system Yb−Si,[14,15] we turned out to investigate the Yb−Ge system. We used equilibrium vapor pressure techniques such as Knudsen effusion weight loss (KEWL) and Knudsen effusion mass spectrometry (KEMS) to investigate the high-temperature decomposition reactions in the composition domains of the Yb−Ge system where two equilibrated solid germanide phases coexist.

In this paper, we report an experimental study concerning the thermodynamic stability of the Yb−Ge phases, complemented by a computational investigation for the Yb_3Ge_5 compound. Experimentally, the high-temperature decomposi-

* Corresponding authors. E-mail: sergio.brutti@uniroma1.it, andrea.ciccioli@uniroma1.it.
[†] Università di Roma-La Sapienza.
[‡] Università di Genova.

10.1021/jp067889b CCC: $37.00
Published on Web 04/20/2007

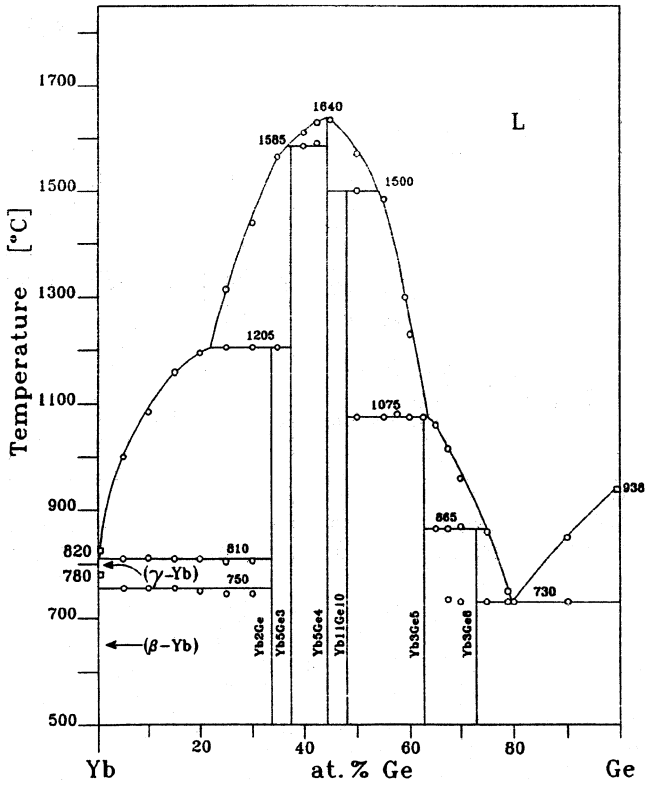

Figure 1. Phase diagram of the Yb−Ge system.

tions of the Yb−Ge intermediate phases were studied by measuring the composition of the gas phase during the high-temperature processes and therefore deriving the decomposition enthalpies of the occurring reactions. The experimental results were used in order to calculate the heats of formation of five out of six of the intermediate phases in the Yb−Ge system. Computationally, the stability of the Yb_3Ge_5(s) compound has been investigated by DFT-LCAO-B3LYP (density functional theory linear combination of atomic orbitals hybrid b3lyp exchange-correlation functional) first principles calculations deriving its equilibrium geometry and the enthalpy of formation at 0 K. The experimental and computational results are discussed together with the available literature.

2. Experimental Section

2.1. Preparation of the Samples. The elemental germanium used was a commercial zone-melting refined product (purity 99.999 wt.%), and ytterbium metal was chosen among several commercially available sources (purity not less than 99.9 wt.%). Bulk Yb−Ge alloys were prepared in a similar way as described in detail in ref 12 for the phase diagram study. Because of the high vapor pressure of ytterbium, the high melting temperatures reached in this system, and the possible reactivity toward the container material, the alloys were prepared with different modalities depending on the germanium concentration of the sample. From 35 to 60 atom% Ge, they were prepared in closed Ta crucibles in a high frequency induction melting furnace. From 60 to 100 atom % Ge, the two elements in proper amounts were directly melted in the induction furnace with a negligible Yb loss. After an annealing procedure, samples were examined by XRD (X-ray diffraction) and SEM-EDS (scanning electron microscopy coupled with electroprobe microanalysis) techniques. Because of the good stability of these alloys toward moist air, no particular care was necessary in their handling. For each alloy sample studied, the vaporization residues (see subsequent section) were subjected to XRD analyses to substantiate the occurrence of the proper equilibrium decomposition processes.

2.2. Vapor Pressure Measurements. For the decomposition equilibria investigated, the vapor pressures were measured with two different tensimetric techniques: KEMS and KEWL. In the KEMS experiments a Nuclide-Patco model 12-60HT single focusing magnetic sector mass spectrometer coupled with a Knudsen cell assembly was used while the KEWL experiments were performed with a Ugine-Eyraud home modified vacuum thermobalance coupled with an effusion cell. The experimental assemblies are essentially the same as what we used in previous works on related intermetallic systems.[14,16,17] Basics of the methods, apparatuses, and data analysis are given in ref 18. Where not otherwise specified, the effusion cells employed were machined from Mo rods 10 mm in diameter and had effusion orifices of 0.5 and 1.0 mm diameter. The cells were heated by means of a graphite cylindrical resistance tube in the case of the thermobalance (isothermal zone height: ∼10 cm) and by means of a tungsten coil resistance in the mass spectrometric measurements: temperatures were measured by a Pt−Pt (10 atom % Rh) thermocouple in the KEWL experiments and by using a disappearing filament optical pyrometer by sighting a blackbody cavity in the bottom of the crucible in the KEMS experiments. In the KEMS experiments, the vapors effusing from the cell were ionized using an emission current of 1 mA and 25−30 eV electron energies, practically at the maximum of the ionization efficiency curve for Yb^+. The pressure calibration procedure for the KEMS measurements was accomplished by performing vaporization of high purity elemental silver.[18]

In the Yb−Ge system, ytterbium is much more volatile than germanium (e.g., for pure elements at $T = 1000$ K, p(Yb) ≈ 10^{-3} bar and p(Ge) ≈ 10^{-13} bar); thus, in the temperature ranges where we studied the vaporization of the alloys in the solid two-phase domains, it was not possible to measure simultaneously the ionic currents of Yb and Ge. Actually, for the Yb-rich solid alloy samples with composition 35−58 atom % Ge, only the Yb^+ ion species could be measured within the sensitivity limit of the mass spectrometer. In the case of Ge-rich alloys with composition 65 and 90 atom % Ge, neither Yb^+ nor Ge^+ could be monitored in the mass spectra so indicating the extremely low activity of Yb in these alloys at temperatures below the transformation temperatures (peritectic and eutectic lines at 1138 and 1003 K, respectively). For all alloys being atomic Yb, the only vapor constituent species, the equilibrium decomposition pressures were generally measured by the KEWL technique. Only in the case of the vaporization of a 51 atom % Ge alloy at temperatures higher than 1075 °C (1348 K) in the region of the solid−liquid equilibrium, we could monitor both Yb(g) and Ge(g). However, because of the very high ytterbium pressure, only a few number of data points could be measured.

3. Computational Method

Unrestricted spin polarized density functional theory calculations were performed on the Yb_3Ge_5(hP8), Ge(diamond), and Yb(fcc) phases using the CRYSTAL2003 code.[19] Within this scheme, the exchange-correlation contributions were calculated by the hybrid functional B3LYP.[20] The CRYSTAL2003 code constructs the periodic Bloch functions for a three-dimensional lattice by the LCAO (linear combination of atomic orbitals) method using localized Gaussian atomic basis with plane-wave phase factors. A k-point Monkhorst-Pack (MP) net, built using

a shrinking factor of 12,[21] has been adopted in all cases for the integration in the reciprocal space. This net corresponds to a mesh of 72 k-points within the irreducible Brillouin zone for the Yb(fcc) and Ge(diamond) lattices and 133 k-points for the Yb_3Ge_5 hP8 lattice. For the Yb(fcc) and Yb_3Ge_5(hP8) phases, in view of their metallic conductor character, also a denser Gilat k-point net was used in the evaluation of the Fermi energy and the density matrix with a shrinking factor of 24, two times the standard MP net, so including 413 and 793 irreducible k-points, respectively. The energy differences with respect to calculations performed with a less dense net of k-points (MP grid with a shrinking factor of 11; Gilat net with a shrinking factor of 22) are smaller than 0.1 kJ mol atom^{-1}.

An all electron 97631/7631/61 Gaussian basis set with polarization functions[22] was adopted for Ge atoms while a pseudopotential approach was used for Yb. To our knowledge, the only optimized pseudopotential basis set for Yb solid-state calculations is a 4f-in-core ECP (effective core potential) by Yang and Dolg[23] with a basis set including 11 electrons in the variational basis (3111/3111/2111 scheme). The latter has been derived from the similar ECP for isolated atomic Yb presented in ref 24 by optimizing the valence basis for crystalline calculations (see ref 23 and section 4.2 for more details). Calculations were also carried out for isolated atomic Yb. In this case, the Gaussian 03 software[25] was used. In this last case, the original extended basis set with the same ECP by Dolg et al.[24] has been adopted together with the same DFT method. It is important to underline that, by using this ECP, the Yb electronic configuration is forced in the trivalent $[4f^{13}]5s^25p^6$-$5d^16s^2$ state whereas this element shows a divalent character as an isolated atom or in the face-centered cubic metallic structure with a $[4f^{14}]5s^25p^66s^2$ ground state configuration.[26]

It is useful to recall that the trivalent/divalent configurations for Yb are originated by the promotion/unpromotion of an in-core 4f electron (4f shell is fully occupied in the ground state electronic configuration of the isolated Yb atoms) to the semi-core 5d shell (completely empty shell in the Yb ground state). Formally, the two electronic configurations for the isolated atom are (1) Yb(divalent), $[Kr]4d^{10}4f^{14}5s^25p^66s^2$, and (2) Yb(trivalent), $[Kr]4d^{10}4f^{13}5s^25p^65d^16s^2$. This simple picture is only univocally defined for isolated atoms were no charge transfer takes place. If we use these concepts to describe solids, only minor changes are necessary: indeed the aforementioned picture is aimed at describing a semi-core electronic configuration that is expected to affect on the bonding characteristics of the Yb atoms within a solid. Indeed in the formation of chemical bonds a trivalent Yb atom could transfer, or mix, up to three ($5d^16s^2$) valence electrons instead of two in the divalent case ($6s^2$). However, even if the effective charge transfer from an Yb atom having a ($5d^16s^2$) valence configuration is less than 3, we can keep on referring to that atom as a trivalent Yb because its semi-core configuration corresponds to the trivalent isolated atomic Yb configuration. The same idea can be applied to the Yb atoms having a ($6s^2$) valence configuration, showing a charge-transfer smaller that 2: in this case, we can definitely refer to these atomic species as divalent Yb atoms regardless of the effective atomic charge.

Finally, lattice parameter optimizations have been performed step-by-step by calculating the minimum in the total energy with respect to each cell parameter to be optimized, starting from the crystallographic data for the three solid phases. At each step, the atomic positional parameters in the Yb_3Ge_5 structure have been relaxed by the optimizing routine implemented in the CRYSTAL2003 code.

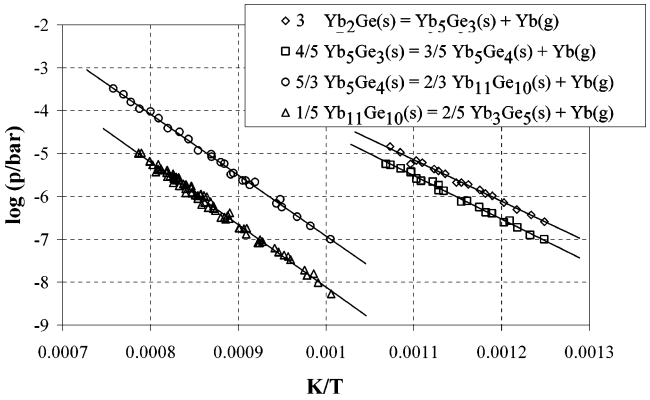

Figure 2. Van't Hoff plots for the high-temperature decomposition reactions of the intermediate phases in the Yb−Ge system.

4. Results and Discussion

4.1. Decomposition Reactions: Equilibrium Pressures and Reaction Enthalpies. As already discussed, below the congruent and incongruent melting temperatures, the intermediate phases in the Yb−Ge system decompose, at high temperature, by loosing gaseous Yb. The generic decomposition reaction for the intermediate phases is given by the following general equation:

$$\frac{z}{zx - wy}\,Yb_xGe_y(s) = Yb(g) + \frac{y}{zx - wy}\,Yb_wGe_z(s)$$

By assuming that the intermediate phases are line compounds, the equilibrium constant for the above processes is given by the partial pressure of Yb(g), that is, $K = p_{Yb}$, bar. The experimental data are reported in Figure 2 in the form of Van't Hoff plots. The linear fitting results for the various experiments and for each reaction are presented in Table 1 together with some experimental details (from now on, the reactions will be identified by the relevant number reported in Table 1).

In the case of reactions 1 and 2, only KEWL experiments were carried out: indeed, in these temperature conditions ($T <$ 800 K) in our KEMS apparatus, the attainment of isothermal conditions along the crucible was difficult to achieve.

In the case of reactions 3 and 4, both KEWL and KEMS techniques have been used. The higher sensitivity of KEMS allowed us to extend the range of measured Yb(g) vapor pressures covering more than 3 orders of magnitude. Moreover, in the case of reactions 3 and 4, several independent experimental runs have been performed. The results for the different runs are presented separately in Table 1 together with the recommended final values that have been obtained by fitting the complete set of experimental data for each reaction. On passing, it can be noted that for reactions 3 and 4, different from the case of reactions 1 and 2, the KEWL measurements could not provide a dataset with more than 12 points, the reason being the large Yb mass loss via the gas phase which rapidly depleted the samples.

Equilibrium pressures have been processed as usual by the second-law method[17] which gives the standard enthalpy of reaction at the average temperature ($\langle T \rangle$) of the experiments as slope of the least-squares fitting line of ln K_{eq} versus $1/T$ data. The enthalpy change at reference room temperature ($\Delta_r H^\circ_{298}$) can then be calculated, provided that the heat capacities C°_p for reactants and products are known. In view of the complete lack of high-temperature experimental heat capacities for ytterbium germanides, the $H^\circ_T - H^\circ_{298}$ values were estimated from 298 K to high temperature by the Kopp-Neumann rule

TABLE 1: Experimental Details and Results of the Linear Fittings of the Vapor Pressure Data for the Studied Reactions

	reaction	%at. Ge	exptl technique	data points	*T*, K range	log p/bar = *A* − *B*/*T* A	*B*·10^{-3}/K
(1)	$3Yb_2Ge(s) = Yb_5Ge_3(s) + Yb(g)$	35	KEWL	18	801−932	5.4980 ± 0.2283	9.6762 ± 0.1977
(2)	$4/5Yb_5Ge_3(s) = 3/5Yb_5Ge_4(s) + Yb(g)$	40	KEWL	21	801−936	5.6515 ± 0.2124	10.150 ± 0.185
(3)	$5/3Yb_5Ge_4(s) = 2/3Yb_{11}Ge_{10}(s) + Yb(g)$	45	KEWL	4	1186−1286		
		45	KEWL	10	1101−1320	7.3669 ± 0.3264	14.492 ± 0.392
		45	KEMS	12	995−1150	7.2225 ± 0.4116	14.245 ± 0.441
		proposed value		26	995−1320	7.1605 ± 0.1416	14.230 ± 0.161
(4)	$1/5Yb_{11}Ge_{10}(s) = 2/5Yb_3Ge_5(s) + Yb(g)$	47.6	KEWL	12	1131−1237	6.6992 ± 0.9385	14.817 ± 1.112
				3	1201−1251		
		51	KEMS	20	994−1210	6.1196 ± 0.2105	14.222 ± 0.231
				20	1014−1194	6.5061 ± 0.3833	14.615 ± 0.428
		58	KEWL	10	1171−1271	6.4439 ± 0.7451	14.539 ± 0.915
				11	1171−1271	6.1146 ± 0.8216	14.187 ± 0.998
		proposed value		76	994−1271	6.4650 ± 0.130	14.578 ± 0.150
(5)	$Yb_{11}Ge_{10}(s) = 11Yb(g) + 10Ge(g)$	51	KEMS	5	1383−1455		
				4	1404−1450		

TABLE 2: Auxiliary Thermal Functions Used in the Second- and Third-Law Data Analysis for the High-Temperature Reactions Studied[a]

T, K	$\Delta_r(H_T^o - H_{298}^o)$ [kJ mol^{-1}] KN rule[b]	G.e.f. [J K^{-1}mol^{-1}] Yb(s)	G.e.f. [J K^{-1}mol^{-1}] Ge(s)	Δ_rG.e.f. [J K^{-1}mol^{-1}] reactions 1−4 KN[b]	Δ_rG.e.f. [J K^{-1}mol^{-1}] reaction 5 m-KN[c]
800	−4.4	70.1	39.9	−110.5	−2626.0
1000	−6.6	74.6	43.6	−109.1	−2616.8
1200	−8.2	78.3	47.0	−108.1	−2609.4
1400	−10.1	81.8	49.9	−107.1	−2602.7
1600	−11.9	84.9	52.5	−106.2	−2594.4

[a] KN = Kopp−Neumann rule; m-KN = modified Kopp−Neumann rule. [b] Calculated for the general reaction $z/(zx - wy)\ Yb_xGe_y(s) = Yb(g) + y/(zx - wy)\ Yb_wGe_z(s)$. [c] Calculated for the reaction $Yb_{11}Ge_{10}(s) = 11Yb(g) + 10Ge(g)$ by assuming for the standard entropies of formation of the $Yb_{11}Ge_{10}(s)$ phase the value −1.0 J K^{-1} mol atom^{-1} (see text for further details).

(KN), that is, as the weighted sum of the heat contents of the constituent elements. Relevant data for Yb and Ge were taken from the IVTANTHERMO compilation[27] (in the case of solid Ge and Yb, the thermodynamic properties above the melting temperatures were estimated by extrapolating data below T_{melt}).

Standard enthalpy changes at 298 K for the decomposition reactions were also tentatively derived by analyzing the equilibrium data with the so-called third-law method[17] using Gibbs energy function (G.e.f.) changes estimated by the KN rule. An overview of the auxiliary thermal functions used in the second- and third-law data analysis is reported in Table 2. In this table, a list of the reaction heat content changes, the extrapolated high-temperature G.e.f. for solid Yb and Ge, and the Δ_rG.e.f. values in the temperature range 800−1600 K estimated by the KN rule are reported for reactions 1−4. In the case of reaction 5, the modified KN estimates (see below for more details) of the Δ_rG.e.f. values used in the analysis are also reported in Table 2 column 6.

The results of both second- and third-law data analyses are reported in Table 3, column 2−4.

Second- and third-law results obtained within the KN approximation are in very good agreement for the decompositions in the Yb_2Ge/Yb_5Ge_3 and Yb_5Ge_3/Yb_5Ge_4 two-phase regions, whereas in the $Yb_5Ge_4/Yb_{11}Ge_{10}$ and $Yb_{11}Ge_{10}/Yb_3Ge_5$ cases a significant discrepancy is observed: in particular, for the $Yb_5Ge_4/Yb_{11}Ge_{10}$ decomposition, we found a difference of about 45 kJ mol^{-1} between second- and third-law determinations. In the lack of experimentally based auxiliary thermodynamic functions, second-law data are generally considered more accurate for this kind of gas−solid equilibria because these are only marginally affected by inaccuracies in the estimation of the heat capacities in the 298 K high-temperature range, and different from the case of the third-law data analysis, the results do not depend on the entropies of formation at 298 K of the involved solid compounds. Thus, second-law values are to be preferred for reactions 1−4 and have been adopted in all of the thermochemical cycles described in the next section in order to derive the heats of formation of the ytterbium germanides.

The study of the decomposition reactions of the other Ge-richer phases (Yb_3Ge_5 and Yb_3Ge_8) was not possible by using our apparatuses owing to the very small volatility of gaseous ytterbium. Indeed, in both cases, Yb(g) and Ge(g) partial pressures were, below the respective incongruent melting temperatures, smaller than the detection limit (10^{-9} bar) of our instruments. This experimental limitation made it impossible to derive the heats of formation of the Yb germanides following the usual self-consistent way (for more details see ref 17) based on the decomposition of a terminal phase (the richest in composition of the less-volatile constituent element) to give a pure element and prompted us to investigate the atomization reaction of $Yb_{11}Ge_{10}(s)$. In the case of the high-temperature decomposition of the sample at 51 atom % Ge, carried out above the $Yb_3Ge_5(s)$ incongruent melting temperature (reaction 5) in the two-phase liquid-$Yb_{11}Ge_{10}$ region, both Yb(g) and Ge(g) were detected in the gas phase, so the thermochemistry of the atomization reaction of the $Yb_{11}Ge_{10}(s)$ phase can be studied

TABLE 3: Vaporization Thermochemistry of the High-Temperature Decomposition Reactions

	reaction	$\Delta_rH_T^\circ$ II law kJ mol^{-1}	$\Delta_rH_{298\ K}^\circ$ II law kJ mol^{-1}	$\Delta_rH_{298\ K}^\circ$ III law[a] kJ mol^{-1}	$\Delta_rH_{298\ K}^\circ$ III law[b] kJ mol^{-1}
(1)	$3Yb_2Ge(s) = Yb_5Ge_3(s) + Yb(g)$	185.1 ± 3.8 at 867 K	190.2 ± 3.8	189.3 ± 0.7	
(2)	$4/5Yb_5Ge_3(s) = 3/5Yb_5Ge_4(s) + Yb(g)$	194.2 ± 3.5 at 871 K	199.4 ± 3.5	195.8 ± 0.8	
(3)	$5/3Yb_5Ge_4(s) = 2/3Yb_{11}Ge_{10}(s) + Yb(g)$	272.3 ± 3.1 at 1141 K	280.0 ± 3.1	235.9 ± 3.7	
(4)	$1/5Yb_{11}Ge_{10}(s) = 2/5Yb_3Ge_5(s) + Yb(g)$	278.9 ± 2.9 at 1155 K	286.7 ± 2.9	261.2 ± 2.2	
(5)	$Yb_{11}Ge_{10}(s) = 11Yb(g) + 10Ge(g)$			6793.2 ± 78.2	6823.1 ± 78.3

[a] Calculated assuming null standard entropies of formation at 298 K, $\Delta_fS_{298K}^\circ$, for all compounds (KN approximation). [b] Calculated assuming for the standard entropy of formation of $Yb_{11}Ge_{10}(s)$ the value, −1.0 J K^{-1} mol atom^{-1} (see text for further details).

TABLE 4: Measured Vapor Pressures of Yb(g) and Ge(g) in Equilibrium over the Two-Phase Region $Yb_{11}Ge_{10}$(s) + Liquid, and the Corresponding Heat of Formation for the $Yb_{11}Ge_{10}$(s) Compound

	T, K	(p(Yb)·10^4) bar	(p(Ge)·10^8) bar	$\Delta_f H^\circ_{298K}$ kJ mol atom^{-1}
run 1	1224	0.06		
	1311	0.33		
	1290	1.0		
	1437	2.8	2.0	−75.0
	1409	2.7	2.1	−69.7
	1385	1.8	1.3	−70.3
	1455	6.9	5.9	−70.3
	1383	1.9	1.9	−70.1
run 2	1436	9.8	3.4	−63.0
	1404	1.9	3.1	−66.3
	1418	1.8	3.4	−69.5
	1450	2.0	4.3	−74.8

directly. The stoichiometry of the relevant atomization process is the following:

$$Yb_{11}Ge_{10}(s) = 11Yb(g) + 10Ge(g)$$

From the latter, we were able to obtain the heat of formation of this phase and, by chain-combining it with the decomposition enthalpies of the other phases, to derive the heats of formation of all of the Yb-richer compounds (see also section 4.3). The summary of the vapor pressures of Yb(g) and Ge(g) measured over the $Yb_{11}Ge_{10}$(s) + liquid region in the course of two independent runs is reported in Table 4 together with three additional data collected in run 1, below the peritectic temperature. These last are collected in the $Yb_{11}Ge_{10}/Yb_3Ge_5$ binary region and compares well, within the typical uncertainty in KEMS experiments, with the corresponding pressures derived by the linear equation of reaction 4 reported in Table 1.

The study of reaction 5 is somewhat challenging from the experimental point of view for several reasons: (i) the high differential of Yb and Ge partial pressures requires the use of conditions where the Yb pressure is not far from the upper limit of the Knudsen molecular flow; (ii) the presence of a liquid phase can favor the occurrence of interaction with the cell material; (iii) the high vaporization rates can quickly change the composition of the sample, depleting the sample in the more volatile (Yb) component and possibly making it cross the boundary with the one-phase (liquid solution) region. In order to approach all of these points, the experiments focused on this reaction were carried out by using different Knudsen cell materials. Indeed, experiments on solid + liquid mixtures were performed testing three different materials: tantalum, a BN−TiB_2 composite, and graphite. The results listed in Table 4 are those obtained using graphite and did not show any appreciable interaction with the sample. Moreover, for all of the experiments, quantitative evaluations of the mass loss were performed in order to check that the boundary limit of the $Yb_{11}Ge_{10}$ + liquid region was not crossed. It is to be noted that data points at $T = 1455$ K (run 1) and $T = 1436$ K (run 2) scatter from the other data, maybe as a consequence of the high pressure of Yb, very close to the upper limit of the Knudsen condition. However, in view of the rather limited number of collected data for this reaction, we retained them in the analysis although these points significantly contribute to the statistical dispersion of the derived thermodynamic quantities. This resulted in a rather generous estimate of the statistical uncertainty associated with the derived formation enthalpy.

The equilibrium constant of the atomization reaction of $Yb_{11}Ge_{10}$ is given by $K = (p_{Yb}/\text{bar})^{11}\cdot(p_{Ge}/\text{bar})^{10}$. Only few data were collected for this process in the course of two independent experiments, trying to reduce the rapid composition change of the sample due to the large partial pressure of Yb(g). The limited number of experimental determinations only allow for a third-law data analysis of the $Yb_{11}Ge_{10}$(s) atomization reaction. The results of the third-law data analysis within the KN approximation for reaction 5 are reported in Table 3, column 4.

It is important to remark that third-law data analysis results are in general sensitive to possible inaccuracies in the evaluation of the G.e.f. of the phases involved in the reactions. As a consequence, in view of the observed discrepancies among second- and third-law results for reactions 3 and 4, an accurate estimate beyond the KN approximation of the G.e.f. for the $Yb_{11}Ge_{10}$(s) phase is to be recommended in order to perform a more reliable third-law analysis of reaction 5. The Δ_rG.e.f. required for the third-law data analysis of the aforementioned atomization process (reaction 5) can be written as:

$$\Delta_r\text{G.e.f.} = \frac{\Delta_r(H^\circ_T - H^\circ_{298})}{T} - \Delta_r(S^\circ_T - S^\circ_{298}) - 10\cdot\Delta_{subl}S^\circ_{298}(Ge) - 11\cdot\Delta_{subl}S^\circ_{298}(Yb) + \Delta_f S^\circ_{298}(Yb_{11}Ge_{10}(s)) \quad (1)$$

$\Delta_r(H^\circ_T - H^\circ_{298})$ and $\Delta_r(S^\circ_T - S^\circ_{298})$ being the heat content and the entropy content changes both referred to 298 K, $\Delta_{subl}S^\circ_{298}(Ge)$ and $\Delta_{subl}S^\circ_{298}(Yb)$ being the sublimation entropies at 298 K of solid Ge and Yb, and $\Delta_f S^\circ_{298}(Yb_{11}Ge_{10}(s))$ being the formation entropy at 298 K for the $Yb_{11}Ge_{10}$(s) phase. Whereas the sublimation terms of the above equation are accurately known and can be easily retrieved from thermochemical compilations,[27] the other addends need to be estimated, owing to the lack of experimental heat capacities in any temperature range for the $Yb_{11}Ge_{10}$(s) phase. The KN rule gives an estimation of the first two terms while within this approximation the $\Delta_f S^\circ_{298}$ ($Yb_{11}Ge_{10}$(s)) is zero. In order to improve the accuracy of Δ_rG.e.f., we tentatively derived an estimation of the entropy of formation of $Yb_{11}Ge_{10}$(s), starting from our experimental data and the literature information available for the thermodynamics of the Yb germanides.

Ahn et al.[5] measured the heat capacities of the Yb_5Ge_4(s) phase in the temperature range 1.8−400 K: from these data, it is possible to calculate the entropy of formation of Yb_5Ge_4(s) at 298 K, $\Delta_f S^\circ_{298}(Yb_5Ge_4(s)) = -3.26 \pm 0.20$ J K^{-1} mol atom^{-1}. By coupling this value with the results of the second-law data analysis for reaction 3, it is possible to derive the entropy of formation for the $Yb_{11}Ge_{10}$(s) phase. Indeed, the intercept of the linear fitting of vapor pressure data for reaction 3 gives the relevant standard entropy change at the average temperature of the experiments, $\Delta_r S^\circ_{1141K}$ (reaction 3) = 137.1 ± 2.9 J K^{-1} mol^{-1}. By reducing this data to 298 K by the KN rule and by using the sublimation entropy at 298 K for Yb(s),[27] that is, $\Delta_{subl}S^\circ_{298}(Yb) = 113.2 \pm 1.0$ J K^{-1} mol^{-1}, and the entropy of formation of the Yb_5Ge_4(s) phase reported above the standard formation entropy for the $Yb_{11}Ge_{10}$(s) phase can be calculated: $\Delta_f S^\circ_{298}(Yb_{11}Ge_{10}(s)) = -1.0 \pm 0.8$ J K^{-1} mol atom^{-1}. Although the derivation of reaction entropies by vapor pressure measurements is generally considered less reliable compared to data derived by the emf technique, this procedure can reasonably be considered to give a better evaluation of $\Delta_f S^\circ_{298}(Yb_{11}Ge_{10}(s))$ compared to the crude KN picture (zero formation entropy). Therefore, the G.e.f. estimation has been modified by considering the nonzero $\Delta_f S^\circ_{298}(Yb_{11}Ge_{10}(s))$ accordingly to the above-reported equation (1). This new set of G.e.f. has been used to perform the third-law data analysis of

TABLE 5: Calculated Equilibrium Structure for the Metallic Yb(fcc), Ge(diamond), and Yb_3Ge_5(hP8) Lattices (Literature Values are Reported in Parentheses)

		cell constants and internal parameters					
phase	lattice	*a*/Å	*c*/Å	x_1	x_2	atomic volume [Å^3]	bulk modulus [GPa]
Yb(s)	fcc	4.9526				30.37	72
		(5.4847)[a]				(41.25)[a]	(31)[d]
Ge(s)	diamond	5.7541				23.81	67
		(5.6575)[b]				(22.64)[b]	(75)[e]
Yb_3Ge_5(s)	hP8	6.9994	4.1267	0.35693	0.74614	21.886	77
		(6.850)[c]	(4.177)[c]	(0.3583)[c]	(0.7410)[c]	(21.23)[c]	

[a] Reference 39. [b] Reference 42. [c] Reference 12. [d] Reference 41. [e] Reference 40.

the experimental vapor pressure data of reaction 5: the result is reported in column 5 of Table 3. This data for the enthalpy of atomization at 298 K of the $Yb_{11}Ge_{10}$(s) phase is to be preferred in comparison with the evaluation obtained by applying the crude KN rule and has been used in the subsequent analysis.

It is to be pointed out that any further third-law data analyses for reactions 1−4 by using the modified-KN G.e.f. sets was not reported, even if, by following the same procedure described for the $Yb_{11}Ge_{10}$(s) phase, all the standard entropies of formation could be easily calculated. Indeed, for these processes (reactions 1−4) the well-assessed second-law values were preferred owing to the lack of independent evaluations of the entropies of formation of the involved phases.

4.2. DFT Energetic Stability of Yb_3Ge_5. DFT total energies of Yb(fcc) and Ge(diamond) have been calculated as well as for the Yb_3Ge_5 phase. Crystal structure optimization results are presented in Table 5 in comparison with the literature data. The optimized lattice parameters are in good agreement with literature for both the Ge(diamond) and the Yb_3Ge_5 phases. However, as expected, the agreement is very poor for the Yb(fcc) structure in which Yb atoms are in fact strictly divalent with a full occupancy of the 4f levels unlike the $4f^{13}$ in core configuration adopted. Indeed, freezing ytterbium atoms to the trivalent configuration leads to a significant underestimate of the lattice parameter (−9.7%).

It can be useful to report a brief comment about the reliability of the adoption of the ECP basis selected for ytterbium in order to predict meaningful results. The ECP adopted here was generated for a quite flexible usage (see ref 24) for both ground states and low excited states with 4f orbitals frozen in core and a strict $5s^25p^65d^16s^2$ trivalent configuration. The use of this ECP provides energetic data for solids in which Yb is in its trivalent core configuration. On the other hand, the flexibility of the ECP and the reliability of the results obtained need to be reconsidered in the combination with the corresponding optimized valence basis set. The adopted basis set used here was developed by Yang and Dolg[23] for a doubly charged Yb cation with a $5s^25p^65d^1$ configuration: as a consequence, this basis set can achieve its best performances if, starting from the neutral atomic configuration with 11 electrons in the valence shell, the Yb charge transfer in the computed system is close to 2. However, small differences between the calculated orbital occupancy of Yb in a compound and the assumed +2 charge of the basis set generation are acceptable and do not alter the reliability of the energetic predictions. In the present case, a good agreement is found between the calculated and the experimental equilibrium structure of the Yb_3Ge_5 compound. Second, the computed Yb charge transfer in the intermetallics phase (i.e., 1.1), although lower than 2, confirms that the semi-core nature of the $5d^1$ electron is not broken in the converged electronic structure. In view of this, the assumed strategy (which, by the way, is the only one available at the moment with the adopted computational method) seems appropriate.

Experimentally, in the Yb_3Ge_5 compound, Yb atoms show a temperature-dependent mixed valence which increases from 2.1 at 4.2 K to approximately 2.3 at 298 K, as ascertained by magnetic susceptivity measurements.[10] Within the frame of the interconfigurational fluctuation model, Grytsiv et al.[10] derived for the Yb_3Ge_5 compound an energy gap between the divalent Yb ground state and the trivalent Yb excited state that is 0.275 eV wide. However, as already mentioned, all of the electronic structure calculations performed involved Yb atoms in the trivalent state. On the other hand, our aim was to derive the enthalpy of formation of the Yb_3Ge_5 phase from elements at the actual valence state (2.3 for Yb in Yb_3Ge_5 and 2.0 for Yb in Yb(fcc)): these are the values that would be accessible by experiments.

Two independent thermodynamic cycles can be considered in order to derive the enthalpy of formation of the Yb_3Ge_5 phase. These can be outlined by referring to the energy levels diagram reported in Figure 3 ("solid-state path" on the left, "gaseous path" on the right of Figure 3), where the various thermodynamic states involved are presented. Only three out of these seven states could be computed by DFT: the respective calculated total energies are represented by the DFT(1), DFT(2), and DFT(3) labels. The energies of these DFT-computed states are related to the other states by four different transition energies namely: $\Delta_{sub}H^\circ_{0K}[Yb^{II}(fcc)]$, $\Delta E[Yb^{II-III}(hP8)]$, $\Delta E[Yb^{II-III}(g)]$, and $\Delta E[Yb^{II-III}(fcc)]$, indicating respectively the sublimation enthalpy of bulk divalent Yb and the Yb divalent−trivalent energy differences for the Yb_3Ge_5(hP8) phase, the isolated gaseous Yb atoms, and the Yb(fcc) phase. The sublimation enthalpy at 0 K of divalent Yb(fcc) was taken from the IVTANTHERMO database,[27] $\Delta_{sub}H^\circ_{0K}[Yb^{II}(fcc)] = 153.0 \pm 5.0$ kJ mol^{-1}, while the Yb divalent−trivalent energy difference for the Yb_3Ge_5(hP8) phase is the aforementioned data

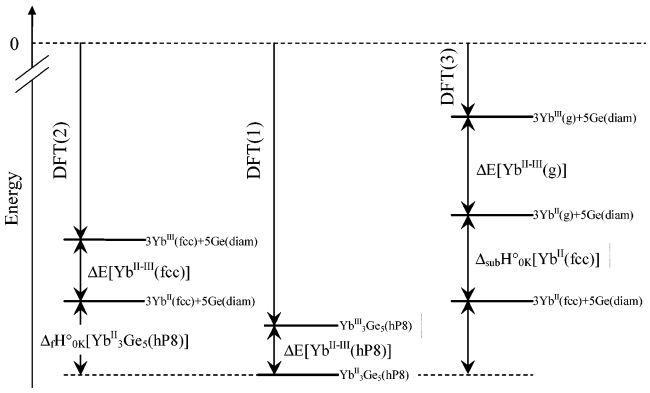

Figure 3. Energy level diagram for the Yb_3Ge_5(hP8), Yb(fcc), Yb(g), and Ge(diamond) states.

measured by Grytsiv et al.,[10] $\Delta E[Yb^{II-III}(hP8)] = 0.275$ eV = 26.5 kJ mol Yb^{-1}.

The isolated gaseous Yb divalent−trivalent energy difference, $\Delta E[Yb^{II-III}(g)]$, is spectroscopically known. However, the trivalent $5s^25p^65d^16s^2$ configuration corresponds to a number of different electronic states and an arbitrary assumption is therefore needed. Considering the lowest transition energy between the Yb $[4f^{14}]5s^25p^66s^2$ and the Yb $[4f^{13}]5s^25p^65d^16s^2$ configurations reported by Martin et al.,[28] the energy difference is 2.87 eV. Dolg and Yang reported a value of 0.44 eV (42.4 kJ mol Yb^{-1}) for the same transition, obtained by an all electron modified HF calculation based on the atomic ECP,[24] for divalent and trivalent Yb from which the trivalent Yb ECP assessed by Yang and Dolg[23] has been derived. This value is significantly smaller compared with the experimental one. In view of a possible compensation of the computational inaccuracies related to the choice of the particular ECP basis set for Yb, we arbitrarily assumed for the $\Delta E[Yb^{II-III}(g)]$ the computational value by Dolg and Yang.

The Yb divalent−trivalent energy difference for the Yb(fcc) phase can be estimated following the approach reported by Gschneidner[29] on the basis of several simple thermochemical cycles using the experimentally known heats of formation of heavy RE solid tri-halogenides (REF_3, $RECl_3$, $REBr_3$, REI_3) and sesquicalchogenides (RE_2O_3, RE_2S_3). We have recalculated this value by using the most recent determinations reported in the literature.[27,30] The resulting mean estimate of the Yb divalent−trivalent energy difference for the Yb(fcc) phase is $\Delta E[Yb^{II-III}(fcc)] = 33.2$ kJ mol Yb^{-1}. This value can be compared with the computational predictions reported by Johansson and co-workers in their series of papers[26,31−37] and in particular with the most recent data[36,37] obtained by DFT-GGA and LDA methods corrected by self-interaction. A mean value of about 48.2 kJ mol Yb^{-1} was proposed by these authors for the solid fcc Yb divalent−trivalent transition energy, somewhat larger than the thermochemical estimate. In conclusion, we adopted the thermochemical estimate for the Yb(fcc) divanlet−trivalent transition energy.

By considering all of these energy differences and the total energies obtained by DFT calculations, the heat of formation of the Yb_3Ge_5 phase with divalent Yb can be finally derived by the following two independent equations (solid-state path and gaseous path, respectively):

$$\Delta_f H^\circ_{0K}[Yb^{II}_3Ge_5(hP8)] = \{DFT(1) - 3\cdot\Delta E[Yb^{II-III}(hP8)]\} - \{DFT(2) - 3\cdot\Delta E[Yb^{II-III}(fcc)]\} \quad (2)$$

$$\Delta_f H^\circ_{0K}[Yb^{II}_3Ge_5(hP8)] = \{DFT(1) - 3\cdot\Delta E[Yb^{II-III}(hP8)]\} - \{DFT(3) - 3\cdot\{\Delta E[Yb^{II-III}(g)] + \Delta_{sub}H^\circ_{0K}[Yb^{II}(fcc)]\}\} \quad (3)$$

The resulting values for the heat of formation of $Yb^{II}_3Ge_5$(hP8) are −58.8 and −65.0 kJ mol $atom^{-1}$, respectively. In view of the above discussion and the arbitrary assumption for the value of the $\Delta E[Yb^{II-III}(g)]$ used in the second cycle ("gaseous path"), the values obtained from the first cycle ("solid-state path") are to be considered more reliable. Owing to this, the solid-state path value has been adopted in the final derivation of the mixed-valence heat of formation of the Yb_3Ge_5 phase, whereas the gaseous path data has been used, in comparison with the previous value, to estimate the overall uncertainty. The final error associated with the solid-state path derivation is therefore calculated as the difference between the two values obtained by eqs 2 and 3. This uncertainty is definitely larger than the computational convergence in the DFT total energies and has been adopted as an estimate of the overall accuracy of the whole thermochemical cycle.

TABLE 6: Heats of Formation (kJ mol $atom^{-1}$) for the Intermediate Phases in the Yb−Ge System

	this study			
phase	experimental	DFT	Miedema model	valence
Yb_2Ge	−66.2 ± 8.3			
Yb_5Ge_3	−69.7 ± 8.2			
Yb_5Ge_4	−73.8 ± 8.2		−58.6	2.4[a]
$Yb_{11}Ge_{10}$	−69.9 ± 8.2			
Yb_3Ge_5	−49.8 ± 13.2	−55.9 ± 6.2	−63.0	2.3[b]
Yb_3Ge_8			−48.5	2.0[c]

[a] Reference 5. [b] Reference 10. [c] Reference 12.

Finally, the mixed valence enthalpy of formation of Yb_3Ge_5 at 298 K, $\Delta_f H^\circ_{298K}(Yb^{mix}_3Ge_5)$, can be derived if any excess contribution to the heat capacities in the 0−298 K temperature range is neglected. To this end, the literature value for the divalent−trivalent Yb transition energy in the Yb_3Ge_5 phase, $\Delta E[Yb^{II-III}(hP8)]$, was used, and the divalent $Yb^{II}_3Ge_5$ ground state occupancy, $\nu(T)$, at 298 K was estimated as reported by Grytsiv et al.[10] The resulting equation is:

$$\Delta_f H^\circ_T(Yb^{mix}_3Ge_5) = \Delta_f H^\circ_{0K}(Yb^{II}_3Ge_5) + 3/8\cdot\Delta E[Yb^{II-III}(hP8)]\cdot(1 - \nu(T))$$

The proposed value for the enthalpy of formation of Yb_3Ge_5 in its "real" mixed valence state at 298 K is $\Delta_f H^\circ_{298K}(Yb^{mix}_3Ge_5) = -55.9 \pm 6.2$ kJ mol $atom^{-1}$.

4.3. Enthalpies of Formation of the Yb−Ge Intermediate Phases. On the basis of the vaporization enthalpies, $\Delta_f H^\circ_{298K}$, presented in columns 4 (reactions 1−4) and 5 (reaction 5) of Table 3, it is possible to calculate, by means of simple thermochemical cycles, a set of formation enthalpies at 298 K for five out of six Yb germanides. Indeed, starting from the atomization enthalpy at 298 K for the $Yb_{11}Ge_{10}$(s) phase (reaction 5), and considering the sublimation enthalpy of pure ytterbium ($\Delta_{sub}H^\circ_{298K}[Yb(s)] = 152.5 \pm 5.0$ kJ mol^{-1})[27] and pure germanium ($\Delta_{sub}H^\circ_{0K}[Ge(s)] = 367.8.0 \pm 5.0$ kJ mol^{-1}),[27] the heat of formation of the $Yb_{11}Ge_{10}$(s) compound can be derived as $\Delta_f H^\circ_{298K}[Yb_{11}Ge_{10}(s)] = -69.9 \pm 7.1$ kJ mol $atom^{-1}$. The heats of formation for the Yb_2Ge(s), Yb_5Ge_3(s), Yb_5Ge_4(s), and Yb_3Ge_5(s) phases can be thereafter derived by using the reaction enthalpy changes at 298 K for decompositions 1 to 4. The results are presented in Table 6 together with the DFT value calculated for the Yb_3Ge_5(s) compound (see previous section) and the estimates obtained by the Miedema model.[38] As the Miedema model requires the knowledge of the valence of the Yb atoms as an imput, we reported Miedema predictions only for the cases, that is, Yb_3Ge_5[10], Yb_3Ge_8[12], and Yb_5Ge_4[5], in which the Yb valence is experimentally known: these predictions were calculated as weighted averages between the divalent and the trivalent cases. Taking also into account the uncertainty associated with experimental values, Miedema's et al. model prediction seems less unaccurate for Yb_3Ge_5 than for Yb_5Ge_4. For the Yb_3Ge_8 phase, the estimate reported here, on the basis of the Miedema et al. predictions and on the preliminary experimental evidence of the divalent character of the Yb atoms in this compound,[12] gives $\Delta_f H^\circ_{298K}[Yb_3Ge_8(s)] = -48.5$ kJ mol $atom^{-1}$. This value appears too negative compared

to the trend of the experimental heats of formation for the other phases of the Yb−Ge system.

For what concerns a DFT prediction, it is to be noted that in comparison with the corresponding experimental data, although the two values agree within the errors, it seems to overestimate the stability of the phase. On the other hand, it compares well with the trend of the other ytterbium germanides whereas, for the same reason, the experimental heat of formation for the Yb_3Ge_5 phase probably slightly underestimates the effective stability of this compound. On the whole, it can be remarked that DFT calculations do not fail in predicting energetic data in acceptable agreement with the experimental value, and this could provide a useful cross check for the transferability of the ECP + basis used for Yb and its application to systems similar to Yb−Ge.

As this is the first reported determination of the heats of formation for the intermediate phases in the Yb−Ge system, no direct comparison with literature is possible. However, in conclusion, it is interesting to note that Yb germanides resulted in being more stable compared with the corresponding silicides.[14] In particular, the experimental heat of formation of the ytterbium silicides for similar stoichiometries are in all cases less negative by about 8−18 kJ mol atom^{-1}. It is to be noted that this energy difference can be found also for other RE germanides in comparison with the corresponding silicides (see as an example data for the La, Ce, Pr, Nd, and Gd cases reported in ref 13). This could be a clue of a systematic difference in the bonding between RE silicides and germanides, probably related to the stronger metallic character of the latter. Further work is needed to investigate this point, mainly focused on the comparative study of the electronic band structures of these compounds.

Acknowledgment. This research project was partially financially supported by the Italian Government in the frame national research project (PRIN, Progetti di rilevante interesse nazionale) “Leghe e Composti Intermetallici: stabilità termodinamica, proprietà fisiche e reattività” funded by the MIUR (Ministero dell’Istruzione, Università e Ricerca). Thanks are also due to Dr. Jun Yang for generously giving us the assessed basis set for the trivalent Yb atom and to Prof. V. K. Pecharsky for kindly providing us with partially unpublished experimental data of the heat capacity of the Yb_5Ge_4 phase. Also, the helpful assistance of Giuseppe Trionfetti in the experiments is acknowledged.

References and Notes

(1) Miller, G. J. *Chem. Soc. Rev.* **2006**, *35*, 799.

(2) Tobash, P. H.; Bobev, S. *J. Am. Chem. Soc.* **2006**, *128*, 3532.

(3) Dallera, C.; Grioni, M.; Shukla, A.; Vankó, G.; Sarrao, J. L.; Rueff, J. P.; Cox, D. L. *Phys. Rev. B: Condens. Matter Mater. Phys.* **2002**, *88*, 196403.

(4) Barla, A.; Chefki, M.; Huhnt, C.; Braden, M.; Leupold, O.; Rüffer, R.; Sanchez, J. P.; Wurth, A.; Mewis, A.; Abd-Elmeguid, M. M. *Phys. Rev. B: Condens. Matter Mater. Phys.* **2004**, *69*, 100102.

(5) Ahn, K.; Tsokol, A. O.; Mozhaervskyi, Yu.; Gschneidner, K. A., Jr.; Pecharsky, V. K. *Phys. Rev. B: Condens. Matter Mater. Phys.* **2005**, *72*, 054404.

(6) Voyer, C. J.; Ryan, D. H.; Ahn, K.; Gschneidner, K. A., Jr.; Pecharsky, V. K. *Phys. Rev. B: Condens. Matter Mater. Phys.* **2006**, *73*, 174422.

(7) Li, R.; Yao, H. B.; Lee, S. J.; Chi, D. Z.; Yu, M. B.; Lo, G. Q.; Kwong, D. L. *Thin Solid Film* **2006**, *504*, 28.

(8) Buyanov, Yu. I.; Velikanova, T. Ya.; Luzan, S. P.; Martsenyuk, P. S.; Polotskaya, R. I.; Sidorko, V. R. *Poroshk. Metall. (Kiev)* **1996**, *99*, 7−8.

(9) Grytsiv, A.; Kaczorowski, D.; Leithe-Jasper, A.; Tran, V. H.; Pikul, A.; Rogl, P. *J. Solid State Chem.* **2002**, *163*, 168.

(10) Grytsiv, A.; Kaczorowski, D.; Leithe-Jasper, A.; Rogl, P.; Potel, M.; Noel, H.; Pikul, A.; Velikanova, T. *J. Solid State Chem.* **2002**, *165*, 178.

(11) Palenzona, A.; Manfrinetti, P.; Brutti, S.; Balducci, G. *J. Alloys Compd.* **2003**, *348*, 100.

(12) Pani, M.; Palenzona, A. *J. Alloys Compd.* **2003**, *360*, 151.

(13) Witusiewicz, V. T.; Sidorko, V. R.; Bulanova, M. V. *J. Alloys Compd.* **1997**, *248*, 233.

(14) Brutti, S.; Balducci, G.; Ciccioli, A.; Gigli, G.; Manfrinetti, P.; Palenzona, A. *Intermetallics* **2003**, *11*, 1153.

(15) Brutti, S.; Balducci, G.; Ciccioli, A.; Gigli, G. *Calphad* **2005**, *29*, 254.

(16) Brutti, S.; Ciccioli, A.; Balducci, G.; Gigli, G.; Borzone, G.; Raggio, R.; Ferro, R. *J. Phase Equilib.* **2002**, *23*, 51.

(17) Brutti, S.; Ciccioli, A.; Balducci, G.; Gigli, G.; Manfrinetti, P.; Napoletano, M. *J. Alloys Compd.* **2001**, *525*, 317−318.

(18) Margrave, J. L. *The Characterization of High-Temperature Vapors;* John Wiley & Sons, Inc.: New York, 1967.

(19) Saunders, V. R.; Dovesi, R.; Roetti, C.; Orlando, R.; Zicovich-Wilson, C. M.; Harrison, N. M.; Doll, K.; Civalleri, B.; Bush, I.; D’Arco, Ph.; Llunell, M. *CRYSTAL2003 User’s manual;* University of Torino: Torino, Italy, 2003.

(20) Becke, A. D. *J. Chem. Phys.* **1993**, *98*, 5648.

(21) Monkhorst, H. J.; Pack, J. D. *Phys. Rev. B: Condens. Matter Mater. Phys.* **1976**, *33*, 1308.

(22) Ruiz, E.; Llunell, M.; Alemany, P. *J. Solid State Chem.* **2003**, *176*, 400.

(23) Yang, J.; Dolg, M. *Theor. Chem. Acc.* **2005**, *113*, 212.

(24) Dolg, M.; Stoll, H.; Savin, A.; Preuss, H. *Theor. Chim. Acta* **1989**, *75*, 173.

(25) Frisch, M. J.; Trucks, G. W.; Schlegel, H. B.; Scuseria, G. E.; Robb, M. A.; Cheeseman, J. R.; Montgomery, J. A., Jr.; Vreven, T.; Kudin, K. N.; Burant, J. C.; Millam, J. M.; Iyengar, S. S.; Tomasi, J.; Barone, V.; Mennucci, B.; Cossi, M.; Scalmani, G.; Rega, N.; Petersson, G. A.; Nakatsuji, H.; Hada, M.; Ehara, M.; Toyota, K.; Fukuda, R.; Hasegawa, J.; Ishida, M.; Nakajima, T.; Honda, Y.; Kitao, O.; Nakai, H.; Klene, M.; Li, X.; Knox, J. E.; Hratchian, H. P.; Cross, J. B.; Bakken, V.; Adamo, C.; Jaramillo, J.; Gomperts, R.; Stratmann, R. E.; Yazyev, O.; Austin, A. J.; Cammi, R.; Pomelli, C.; Ochterski, J. W.; Ayala, P. Y.; Morokuma, K.; Voth, G. A.; Salvador, P.; Dannenberg, J. J.; Zakrzewski, V. G.; Dapprich, S.; Daniels, A. D.; Strain, M. C.; Farkas, O.; Malick, D. K.; Rabuck, A. D.; Raghavachari, K.; Foresman, J. B.; Ortiz, J. V.; Cui, Q.; Baboul, A. G.; Clifford, S.; Cioslowski, J.; Stefanov, B. B.; Liu, G.; Liashenko, A.; Piskorz, P.; Komaromi, I.; Martin, R. L.; Fox, D. J.; Keith, T.; Al-Laham, M. A.; Peng, C. Y.; Nanayakkara, A.; Challacombe, M.; Gill, P. M. W.; Johnson, B.; Chen, W.; Wong, M. W.; Gonzalez, C.; Pople, J. A. *Gaussian 03*, revision C.02; Gaussian, Inc.: Wallingford, CT, 2004.

(26) Strange, P.; Svane, A.; Temmerman, W. M.; Szotek, Z.; Winter, H. *Nature* **1999**, *399*, 756.

(27) Iorish, V. S.; Belov, G. V.; Gurvich, L. V.; Yungman, V. S. *IVTANTHERMO for Windows − Thermodynamic database and thermodynamic modelling software;* Glushko Thermocenter of Russian Academy of Sciences: Moskow, Russia, 2005.

(28) Martin, W. C.; Zalubas, R.; Hagan, L. *Atomic Energy Levels - The Rare-Earth Elements;* NSRDS-NBS, US Government Printing Office: Washington, DC, 1978.

(29) Gschneidner, K. A., Jr. *J. Less-Common Met.* **1969**, *17*, 13.

(30) Gschneidner, K. A., Jr.; Bunzli, J. C.; Pecharsky, V. *Handbook of the Physics and Chemistry if Rare Earths*, Vol. 33; North Holland, Amsterdam, The Netherlands, 2003.

(31) Johansson, B.; Rosengren, A. *Phys. Rev. B: Condensed Matter Mater. Phys.* **1975**, *11*, 2836.

(32) Johansson, B.; Munck. P. *J. Less-Common Met.* **1984**, *100*, 49.

(33) Johansson, B. *Phys. Rev. B: Condensed Matter Mater. Phys.* **1979**, *20*, 1315.

(34) Eriksson, O.; Brooks, M. S. S.; Johansson, B. *J. Less-Common Met.* **1990**, *158*, 207.

(35) Delin, A.; Fast, L.; Johansson, B.; Eriksson, O.; Wills, J. M. *Phys. Rev. B: Condensed Matter Mater. Phys.* **1998**, *58*, 4345.

(36) Delin, A.; Fast, L.; Johansson, B.; Wills, J. M.; Eriksson, O. *Phys. Rev. Lett.* **1997**, *79*, 4637.

(37) Temmerman, W. M.; Szotek, Z.; Svane, A.; Strange, P.; Winter, H.; Delin, A.; Johansson, B.; Eriksson, O.; Fast, L.; Wills, J. M. *Phys. Rev. Lett.* **1999**, *83*, 3900.

(38) De Boer, F. R.; Boom, R.; Mattens, W. C. M.; Miedema, A. R. *Cohesion in Metals - Transition Metal Alloys;* North Holland: Amsterdam, The Netherlands, 1988.

(39) Harris, I. R.; Raynor, G. V. *J. Less-Common Met.* **1969**, *17*, 336.

(40) Levinstein, M. *Handbook series on semiconductor parameters*, Vols. 1 and 2; World Scientific: London, U.K., 1999.

(41) Lide, D. R. *Chemical Rubber Company handbook of chemistry and physics*; CRC Press: Boca Raton, FL, 1998.

(42) Singh, H. P. *Acta Crystallogr.* **1968**, *24A*, 469.